Stoichiometry and deletion analyses of subunits in the heterotrimeric F-ATPase *c* ring from the acetogenic bacterium *Acetobacterium woodii*

Karsten Brandt[1], Daniel B. Müller[1#], Jan Hoffmann[2], Julian D. Langer[3], Bernd Brutschy[2], Nina Morgner[2], Volker Müller[1*]

[1]Molecular Microbiology & Bioenergetics, Institute of Molecular Biosciences, Goethe University Frankfurt/Main, Max-von-Laue-Str. 9, 60438 Frankfurt, Germany

[2]Institute for Physical and Theoretical Chemistry, Goethe University Frankfurt/Main, Max-von-Laue Str. 7, 60438 Frankfurt, Germany

[3]Department of Structural Biology, Max-Planck-Institute of Biophysics, Max-von-Laue-Str. 3, 60438 Frankfurt am Main, Germany

[#]current address: Institute of Microbiology, ETH Zurich, Vladimir-Prelog-Weg 4, 8093 Zurich, Switzerland

To whom the correspondence should be addressed: Volker Müller, Molecular Microbiology & Bioenergetics, Institute of Molecular Biosciences, Johann Wolfgang Goethe University Frankfurt/Main, Max-von-Laue-Str. 9, 60438 Frankfurt, Germany. Phone: +49-69-79829507, Fax: +49-69-79829306, Electronic mail address: vmueller@bio.uni-frankfurt.de

Keywords: ATPase, sodium transport, membrane enzyme, bioenergetics, liposome, hybrid rotor, *c* subunit

Abstract

The ion-translocating *c* ring of the Na^+ F_1F_o ATP synthase of the anaerobic bacterium *Acetobacterium woodii* is the first heteromeric *c* ring found in nature that contains one V- (c_1) and two F-type like *c* subunits (c_2/c_3), the latter of identical amino acid sequence. To address whether they are of equal or different importance for function, they were deleted in combination or individually. Deletion of c_1 was compensated by incorporation of two c_2/c_3 subunits but the enzyme was unstable and largely impaired in Na^+ transport. Deletion of c_2 was compensated by incorporation of c_3 but also led to a reduction of Na^+ transport. Deletion of c_3 had no effect. In contrast, deletion of both c_2 and c_3 led to a complete loss of ATPase activity at the cytoplasmic membrane. Mass spectrometric analysis of c_2+1 Ala and c_2+2 Ala variants revealed a copy number of 8:1 for c_2:c_3 which is consistent with the biochemical characteristics of the variants. These data indicate a role of c_1 in assembly and a function of c_2 as predominant *c* ring constituent.

Introduction

The anaerobic acetogenic bacterium *Acetobacterium woodii* is the prime example for an organism that uses Na^+ as coupling ion for chemiosmotic energy conservation [1-5]. The energy conserving pathways such as carbonate (Wood-Ljungdahl pathway) and caffeate respiration have the same coupling site, a Na^+-translocating ferredoxin:NAD^+ oxidoreductase (Rnf complex) [6-12] and the electrochemical sodium ion potential established by the Rnf complex then drives ATP synthesis by a Na^+ F_1F_o ATP synthase [13, 14].

The Na^+ F_1F_o ATP synthase of *A. woodii* is encoded by the *atp* operon that has a unique genetic organization [15-18]. Instead of one gene encoding the rotor subunit *c*, the operon contains three tandemly organized genes each encoding a *c* subunit. *atpE₁* encodes an 18 kDa protein with four transmembrane helices and one additional N-terminal helix, but only one ion

binding site and thus, is similar to the *c* subunit of V_1V_o ATPases. *atpE2* and *atpE3* code for identical, 8 kDa *c* subunits with one ion binding site in two transmembrane helices, typical for F_1F_o ATPases. Both types of subunits are produced (c_1 and $c_{2/3}$) and present in the *c* ring of *A. woodii* making it the first F_oV_o hybrid rotor found in nature [19]. Most interestingly, the F_oV_o hybrid rotor-containing enzyme is capable of ATP synthesis [14].

The hybrid rotor was purified and shown by laser induced liquid beam ion desorption mass spectrometry (LILBID-MS) to contain subunits $c_{2/3}$:c_1 in a stoichiometry of 9:1. This stoichiometry was independent of the carbon source of the growth medium [20]. A recent high resolution structure at 2.1 Å confirmed the 9:1 stoichiometry and the absence of the second Na^+ binding site in c_1 [21]. Moreover, the N-terminal helix was shown to be present across the central pore towards a distal $c_{2/3}$ subunit, parallel to the membrane plane [21]. To address the role of the different *c* subunits in the hybrid rotor, we have expressed the *atp* operon in *E. coli*, produced and analyzed the ATPase and studied the effect of deletions of single *c* subunits or combinations on ATP hydrolysis, Na^+ transport and assembly.

Results

Truncation of the N-terminal helix of subunit c_1 of the Na^+ F_1F_o ATP synthase of *A. woodii* has no effect on assembly or activity

The N-terminal helix of subunit c_1 was suggested before to be involved in *c* ring assembly and/or function [15, 21]. To address this hypothesis, the N-terminal helix of subunit c_1 was truncated (æ2-18) (Fig. 1) and the ATP synthase was purified as described previously [22]. The ATPase activity of the purified enzyme was 6.2 U/mg protein which is in the same range as the wild type enzyme. The enzyme was reconstituted into liposomes and Na^+ transport was measured (Fig. 2A). The rate of Na^+ transport catalyzed by the variant was 775 ± 27 nmol Na^+/min Āmg protein corresponding to a Na^+/ATP stoichiometry of 0.26 ± 0.1 which is comparable to the wild type enzyme (0.27 ± 0.1). Deletion of the N-terminal helix had no effect on the *c* ring composition as judged by SDS gel electrophoresis and LILBID-MS of the purified

c ring (Fig. 2).

Subunit c_1 and c_2 but not c_3 are crucial for incorporation of the ATP synthase into the cytoplasmic membrane

To analyze the importance of the individual *c* subunits in incorporating the ATP synthase into the cytoplasmic membrane, they were deleted. The plasmids encoding deletion variants of the ATPase were constructed as described in experimental procedures with the plasmid pKB3-His as template. The design of the primers to delete either only *atpE*$_2$ or only *atpE*$_3$ was problematic due to 92.8% DNA sequence identity of the two genes. Therefore, the primers were designed to bind in the intergenic region which is less conserved. The plasmids constructed were transformed in the ATP synthase negative *E. coli* strain DK8 and cells were cultivated as described previously [22]. To monitor incorporation of the enzyme into the cytoplasmic membrane, the amounts of subunits *b* and β were detected by immunoblotting. The anti subunit *b* antibody also recognizes a 15 kDa peptide, most likely a degradation product whose concentration is higher in the deletion variants. Deletion of either *atpE*$_1$, *atpE*$_2$ or *atpE*$_3$ had no effect on the amounts of subunits *b* and ϐ present in the cytoplasmic membrane (Fig. 3A, B), whereas deletion of *atpE*$_2$ and *atpE*$_3$ led to a drastically reduced amount of subunit *b* and the complete absence of subunit ϐ (Fig. 3A, B). The ATPase activity of the variants missing c_1 or c_2 was reduced by nearly 70% whereas deletion of c_3 had no effect on ATPase activity (Fig. 3C). The complete loss of incorporation of ATP synthases into the cytoplasmic membrane in the *atpE*$_2$/*atpE*$_3$ deletion indicates that a c_1 ring is not produced or not stable. Production of a ring consisting only of c_1 could be sterically inhibited since each monomer has an N terminal extension which is perpendicular to the *c* ring in the wild type. To address this possibility, the sequence encoding the N-terminal helix was deleted as described before in the $\Delta c_{2/3}$ variant. However, ATP synthase was still not incorporated into the cytoplasmic membrane (Fig. 3A, B).

Subunit composition of *c* rings in the variants

To analyze the *c* ring composition, the wild type enzyme and the variants were solubilized from the cytoplasmic membrane and purified in one step *via* affinity chromatography (Fig. 3D). In contrast to the wild type and the æc_3 variant, the æc_1 and æc_2 variants had less c ring. Moreover, the amount of subunit ε was apparently reduced in the æc_1 variant. Consistent with the ATPase activities found at the cytoplasmic membrane, the ATPase activity of the æc_3 variant was comparable to the wild type enzyme with 7.0 U/mg whereas the æc_1 and æc_2 variants only had activities of 1.7 and 2.7 U/mg, respectively (Fig. 3E). The *c* ring was then purified from the variants as described [20]. The *c* ring purified from the æc_1 variant still had the SDS-resistant phenotype (Fig. 4A and B). After dissociation of the *c* ring with trichloroacetic acid, monomeric subunits $c_{2/3}$ became visible but not subunit c_1. The *c* rings of the æc_2 or æc_3 variant also had the SDS-resistant phenotype and contained the monomeric $c_{2/3}$ and c_1 subunits. To reveal the stoichiometry of the *c* subunits in the *c* rings from the variants, LILBID-MS analyses under medium laser desorption conditions were performed. Under these conditions the intact *c* ring as well as the fragmentation of the *c* ring could be detected. In the æc_2 variant, the c_3:c_1 stoichiometry was 9:1, in the æc_3 variant it was 9 c_2: 1 c_1 (Fig. 4C and 4D). Apparently, c_2 and c_3 are exchangeable. The *c* ring of the æc_1 variant apparently contained 11 copies of the $c_{2/3}$ subunit (Fig. 4E), indicating that the loss of c_1 is compensated for by incorporation of two $c_{2/3}$ subunits.

The æc_1 variant is impaired in Na^+ transport

To determine whether the variants are still able to translocate Na^+, the purified ATP synthases were reconstituted into liposomes. After the addition of ATP to the proteoliposomes, incubated in the presence of 4.5 mM $^{22}Na^+$, sodium ions were transported into the lumen of the proteoliposomes (Fig. 5A). The Na^+ transport rate of the æc_3 variant was again comparable to the wild type with 835 ± 45 nmol/ min Ämg protein, corresponding to a Na^+/ATP stoichiometry of 0.29 ± 0.02. The rate of Na^+ transport of the æc_2 variant was lower than the wild type with

318 ± 79 nmol/ min Āmg protein, corresponding to a Na^+/ATP stoichiometry of 0.19 ± 0.02. The lowest Na^+ transport rate with <1% of the wild type was found for the enzyme from the æc_1 variant (6.5 ± 0.8 nmol/ min Āmg protein, corresponding to a Na^+/ATP stoichiometry of 0.009 ± 0.1), concluding that Na^+ transport in this variant is nearly completely abolished.

Deletion of *atpE*$_1$ ï *atpE*$_3$ does not reduce transcription of the ATPase genes

The result that deletion of *atpE*$_2$ but not *atpE*$_3$ had an effect on the properties of the ATP synthase, although both proteins are 100% identical, could possibly be attributed to a polar effect of the deletion on expression of downstream genes. To this end, we quantified expression levels of downstream genes by quantitative real time PCR. The relative mRNA level were determined for the *atpB* gene, which is directly in front of the *atpE* genes, the *atpF* gene, which is the gene after the *atpE* genes, and the *atpD* which is close to the end of the *atp* operon. As can be seen from Fig. 5B, neither deletion of *atpE*$_1$ nor *atpE*$_2$ or *atpE*$_3$ reduced the mRNA levels of *atpB*, *atpF* or *atpD*. This experiment proves that the effect of the deletion of *atpE*$_2$ is not caused by reducing the transcript level of downstream genes.

Subunit *c*$_2$ dominates over *c*$_3$ in the *c* ring

To analyze whether there is a translational regulation which could explain the differences in the æc_2 and æc_3 variants the ratio of the two subunits in the *c* rings was determined. Since subunits c_2 and c_3 are 100% identical in their amino acid sequence, individual subunits were uniquely tagged by addition of one or two alanine residues at the C-terminal end. The different enzyme variants were purified and showed ATPase activities comparable to the wild type enzyme. The *c* monomers were extracted from the enzymes. As shown in Fig. 6 the MALDI-TOF-MS analysis of the wild type revealed only one major peak with a molecular mass of 8.18 kDa representing the mass of the subunits c_2 and c_3. The additional peaks are due to cation adduct peaks ($[M+nNa^+]^+$) and chemical modifications such as oxidation and formylation. In the case where the c_2 subunit was tagged with one alanine (c_2+1A) the major peak was shifted to a mass of 8.25 kDa representing the molecular mass of the c_2+1A subunit. A small peak was still

obtained at 8.18 kDa which corresponds to the c_3 subunit. When c_2 was tagged with two alanine residues (c_2+2A), the major peak was shifted to a molecular mass of 8.32 kDa corresponding to the c_2+2A monomer. Again, the non-modified c_3 subunit was still visible at 8.18 kDa. The analyses of the c_3 variant with an additional alanine (c_3+1A) showed that the major peak remains at a molecular mass of 8.18 kDa which represents in this case the c_2 subunit. The expected peak of a c_3+1A subunit with a mass of 8.25 kDa is not clearly visible due to its low intensity compared to the c_2 adduct peaks (see above). To determine the ratio of c_2:c_3 the area under the peaks was analyzed. These results show that subunit c_2 represent 92.43±1.05% of the F-type like *c* subunits. Based on the known stoichiometry of 9:1 ($c_{2/3}$:c_1), the stoichiometry of c_1:c_2:c_3 can be calculated to 1:8.3:0.7.

Discussion

The recently published procedure to produce the Na^+ F_1F_o ATP synthase of *A. woodii* heterologously in *E. coli* [22] was used to determine the role of the N-terminal helix of subunit c_1 and the role of the different *c* subunits within the F_oV_o hybrid rotor. The hybrid rotor of *A. woodii* is unique since it contains one V-type like *c* subunit (c_1) and nine copies of F-type like *c* subunits (c_2 and c_3). Previous analysis revealed that the c_1 subunit contains an additional N-terminal helix [15] and the recently solved structure of the *c* ring revealed that this helix is oriented across the central pore of the ring on the periplasmic site [21]. A similar N-terminal helix had been observed for the *c* ring of the V-type ATPase from *Saccharomyces cerevisiae*. This enzyme is also a heteromer consisting of three different V-type subunits, *c*, *c*ô and *c*ôô [23-25]. The *c* and *c*ô subunits have four transmembrane helices, whereas *c*ôô has four transmembrane helices and the additional N-terminal helix [24] which lies on the cytoplasmic site of the membrane [23]. Deletion of this helix had no effect on the V-type ATPase activity as well as on proton translocation and the truncated version of *c*ôô can complement the loss of the full length *c*ôô protein [23]. Due to the orientation of the helix an interaction with the V_1 part of the enzyme was suggested to increase the stability of the complex but this could not be

confirmed during the study [23]. Similarly, we observed neither an effect on enzyme activity nor on *c* ring stoichiometry when the N-terminal helix was deleted.

The deletion of the single *atpE* genes had no effect on the transcription or translation of the other ATP synthase genes of *A. woodii*. Therefore, polar effects of the deletions on expression of downstream genes can be excluded. The double deletion mutant (æ$atpE_2$/$atpE_3$) was not able to build an intact ATP synthase presumably due to a not assembled *c* ring which is known as the assembly platform of the ATP synthase [26, 27]. To exclude a steric effect by the N-terminal helix of the c_1 subunit during assembly of a potential c_1 ring the helix was deleted in the double mutant but the result was still the same. It was possible to purify the single deletion variants of the ATP synthase, but protein yield, activity and subunit composition differed. The deletion of the $atpE_3$ gene had almost no effect and the enzyme displayed characteristics comparable to the wild type. In contrast, the deletion of the $atpE_2$ gene led to an enzyme with less than 50% activity compared to the wild type. For both deletion variants the *c* ring stoichiometry could be determined and it was the same 9:1 ($c_{2/3}$:c_1) stoichiometry as in the wild type. The deletion of the V-type like *c* subunit had the largest effect. Although the loss of c_1 was compensated by two $c_{2/3}$ subunits, the purified enzyme had the lowest ATPase activity and was inactive in Na^+ transport indicating that c_1 is essential for correct assembly of the functional *c* ring. In addition, it was very unstable resulting in a drastic reduction in yield. Comparison of LILBID measurements of all *c* rings under same desorption conditions showed that $(c_{2/3})_{11}$ rings are less stable if compared to the others. Based on the high resolution structure it was speculated that the c_1 subunit is a potential binding site of the central stalk [21]. The cytoplasmic site of the *c* ring is largely electronegative, due to a glutamate residue of the cytoplasmic loops of the $c_{2/3}$ subunits. Surprisingly, the cytoplasmic surface of the c_1 subunit is electropositive and this may enhance the interaction with subunit ε and γ in which potential interaction sites with more electronegative residues are observed. This is consistent with the reduced amount of subunit ε in the Δc_1 variant.

In the case of the heteromeric *c* ring of the V-ATPase of *S. cervisiae* all three *c* subunits

are essential and cannot be substituted by each other [23]. In the case of the *A. woodii c* ring only the c_1 and c_2 subunit are essential for a functional ATP synthase. This is consistent with the observation that c_3 is only a minor fraction in the ring (6%). Since $atpE_2$ and $atpE_3$ are encoded by one transcriptional message and are 100% identical on the amino acid level, it is not obvious why their relative proportions in the *c* ring are significantly different. A regulation on the translational level may be present. Although the ribosome binding sites in front of both genes are identical, the difference in regulation can be due to different translation initiation regions (TIR) which are known to be involved in the translational regulation of genes in the *atp* operon [28]. The TIR is defined as a specific mRNA region which is significantly larger than the region of the Shine-Dalgarno sequence and the start codon [29, 30]. The TIR is not only upstream of the start codon but also downstream [31] and the regulation is due to different secondary structures of these mRNA regions [28]. Different translation rates from one transcriptional message may be the molecular basis for the different copy numbers of subunits in holoenzyme complex. In *E. coli*, the strongest TIR of the *atp* operon is in front of the *atpE* gene [32, 33], whereas the weakest is the one of *atpI* followed by the one of *atpB* [32, 34]. The TIR of *atpD* for example is four times weaker as the one of *atpE* [33]. Besides these individual TIRs, translational coupling also plays a significant role in gene expression, especially in the middle of the *atp* operon [33].

Based on the different effects of the deletions one can conclude that c_1 alone is not able to assemble into a stable *c* ring. c_1 may be the assembly platform on which c_2 is mounted. c_2 and c_3 are 100% identical proteins but only 7.57±1.05% of the F-type like *c* subunits are made by c_3. The loss of this fraction is not detrimental for assembly and function. On the other hand the results show that the loss of 92.43±1.05% of the F-type like *c* subunits in the æc_2 mutant is severe for the enzyme activity. If the loss of activity is due to a mixture of correctly assembled and misassembled ATP synthases without a *c* ring due to lower amounts of *c* subunits available needs further investigation. Whether the amount of the F-type like *c* subunits and the effect of deletions is the same in the native host cannot be answered at the moment due to a lack of a genetic system for *A. woodii*. Anyway, although database searches suggest the presence of c_1/c_2

hybrid rotors in other bacteria the *c* ring from *A. woodii* is so far the only with three different protomers [18]. This observation is also in line with the finding that deletion of $atpE_3$ in *A. woodii* is without consequence.

Experimental procedures

Construction of expression vectors for the mutants of the *A. woodii* Na^+ F_1F_o ATP synthase

All DNA modifying procedures were performed according to standard methods [35]. The plasmid pKB3-His contains the *A. woodii* $atpIBE_1E_2E_3FHAGDC$ operon and encodes a His_6-tag at the N-terminus of subunit ϐ [22]. All mutants are derived from plasmid pKB3-His. The primers (Tab. 1) for the deletion mutants were phosphorylated and after the amplification the fragment was ligated. For the introduction of additional alanine residues at the C-terminus of subunit c_2 or c_3 the primers contained the corresponding additional codon for alanine.

Cell growth, overproduction and purification of the Na^+ F_1F_o ATP synthase

E. coli DK8 (æ*atpB-C*) [36] harboring the plasmids were cultivated as described previously [22]. The overproduction and purification was done as described previously [22].

Determination of ATPase activity, purification of the *c* ring, LILBID-MS of the *c* rings, reconstitution of the ATP synthase in proteoliposomes and measurement of Na^+ translocation

Determination of ATPase activity, purification of the *c* ring, LILBID-MS of *c* rings, reconstitution of the ATP synthase in proteoliposomes and measurement of Na^+ translocation were performed as described previously [22].

RNA purification, cDNA synthesis and quantitative real time PCR

Total RNA from *E. coli* containing the plasmids of the wild type and the deletion mutants was prepared using Invitrap Spin Cell RNA kit (STRATEC Molecular, Berlin) according to the

manufacturerôs instructions. Total RNA was collected from samples in duplicates after the induction with IPTG for 1.5 h. 2 µg of total RNA were reverse transcribed in a total volume of 50 εl containing 50 U reverse transcriptase (Promega) for 50 min at 50°C according to the manufacturerôs instructions. The cDNA levels were subsequently analyzed using a Rotor-Gene RG 3000 Real Time DNA Detection System (Corbett Research Cambridge, United Kingdom). Each sample was measured in triplicates in a reaction mixture (25 εl final volume) containing 1× ABsolute QPCR SYBR Green Mix (Thermo Scientific, Surrey, UK) and 400 nM primer mix (Tab. 2). The threshold cycles (Ct) were calculated using Rotor Gene 6.0 Software. All real-time PCR quantifications were performed simultaneously with the housekeeping gene CysG [37] and no-template controls.

Chloroform/methanol extraction of *c* subunits and MALDI-TOF-MS measurements

For the removal of salt and detergent the purified ATP synthases were treated with C4 Zip Tips according to [38]. Therefore the C4 matrix (bed volume, 0.6 µl) of a 10-µl Zip Tip was first equilibrated with 20 µl of 100% acetonitrile and 20 µl of 0.1% trifluoroacetic acid. ATP synthase was coupled to the equilibrated matrix and washed with 30 µl of 0.1% trifluoroacetic acid. The F_1F_o ATP synthase was eluted with 10 µl of 90% acetonitrile in 0.1% trifluoroacetic acid. The ATP synthase and the *c* ring of *A. woodii* were disintegrated into *c* monomers by the addition of 10 µl chloroform/methanol (2:1, v/v) as described previously [38]. The solution containing the *c* monomers were dried by vacuum evaporation for 1.5 h at room temperature. The dried protein pellet was mixed with 1 µl of 2,5-dihydroxyacetophenone matrix (15 mg/ml 2,5- dihydroxyacetophenone in 75% ethanol in 20 mM sodium citrate; Bruker Daltonics) and spotted on ground steel target plates (Bruker Daltonics). MALDI mass spectra were recorded in a mass range of 5ï 20 kDa using a Bruker Autoflex III Smartbeam mass spectrometer. Detection was optimized for *m*/*z* values between 5 and 20 kDa and calibrated using calibration standards (protein molecular weight calibration standard 1; Bruker Daltonics).

Acknowledgements

This work was supported by grants from the Deutsche Forschungsgemeinschaft (SFB 807 to VM), the ESFRI-Instruct Initiative of the European Union (JL), and the European Research Council under the European Union's Seventh Framework Programme (FP7/2007-2013) / ERC Grant agreement n° 337567 (NM).

Author contribution

K.B., D.B.M., J.D.L., B.B., N.M., and V.M. designed research; K.B., D.B.M., J.H. and J.D.L. performed research; K.B., J.H., J.D.L., N.M., and V.M. analyzed data; K.B., J.D.L., N.M., and V.M. wrote the paper.

References

1. Müller, V., Imkamp, F., Rauwolf, A., Küsel, K. & Drake, H. L. (2004) Molecular and cellular biology of acetogenic bacteria in *In: Strict and facultative anaerobes Medical and environmental aspects* (Nakano, M. M. & Zuber, P., eds) pp. 251-281, Horizon Biosciences, Norfolk.

2. Müller, V. (2003) Energy conservation in acetogenic bacteria, *Appl Environ Microbiol.* **69**, 6345-6353.

3. Schmidt, S., Biegel, E. & Müller, V. (2009) The ins and outs of Na^+ bioenergetics in *Acetobacterium woodii*, *Biochim Biophys Acta.* **1787**, 691-696.

4. Müller, V., Aufurth, S. & Rahlfs, S. (2001) The Na^+ cycle in *Acetobacterium woodii*: identification and characterization of a Na^+-translocating F_1F_O-ATPase with a mixed oligomer of 8 and 16 kDa proteolipids, *Biochim Biophys Acta.* **1505**, 108-120.

5. Schuchmann, K. & Müller, V. (2014) Autotrophy at the thermodynamic limit of life: a model for energy conservation in acetogenic bacteria, *Nat Rev Microbiol.* **12**, 809-821.

6. Heise, R., Müller, V. & Gottschalk, G. (1989) Sodium dependence of acetate formation by the acetogenic bacterium *Acetobacterium woodii*., *Journal of Bacteriology.* **171**, 5473-5478.

7. Heise, R., Müller, V. & Gottschalk, G. (1993) Acetogenesis and ATP synthesis in *Acetobacterium woodii* are coupled *via* a transmembrane primary sodium ion gradient, *FEMS Microbiol Lett.* **112**, 261-268.

8. Imkamp, F. & Müller, V. (2002) Chemiosmotic energy conservation with Na^+ as the coupling ion during hydrogen-dependent caffeate reduction by *Acetobacterium woodii*, *Journal of Bacteriology.* **184**, 1947-1951.

9. Biegel, E. & Müller, V. (2010) Bacterial Na^+-translocating ferredoxin:NAD^+ oxidoreductase, *Proc Natl Acad Sci USA.* **107**, 18138-18142.

10. Biegel, E., Schmidt, S., González, J. M. & Müller, V. (2011) Biochemistry, evolution and physiological function of the Rnf complex, a novel ion-motive electron transport complex in

prokaryotes, *Cell Mol Life Sci.* **68**, 613-634.

11. Poehlein, A., Schmidt, S., Kaster, A.-K., Goenrich, M., Vollmers, J., Thürmer, A., Bertsch, J., Schuchmann, K., Voigt, B., Hecker, M., Daniel, R., Thauer, R. K., Gottschalk, G. & Müller, V. (2012) An ancient pathway combining carbon dioxide fixation with the generation and utilization of a sodium ion gradient for ATP synthesis, *PLoS One.* **7**, e33439.

12. Hess, V., Schuchmann, K. & Müller, V. (2013) The ferredoxin:NAD^+ oxidoreductase (Rnf) from the acetogen *Acetobacterium woodii* requires Na^+ and is reversibly coupled to the membrane potential, *J Biol Chem.* **288**, 31496-31502.

13. Heise, R., Müller, V. & Gottschalk, G. (1992) Presence of a sodium-translocating ATPase in membrane vesicles of the homoacetogenic bacterium *Acetobacterium woodii*, *Eur J Biochem.* **206**, 553-557.

14. Fritz, M. & Müller, V. (2007) An intermediate step in the evolution of ATPases - the F_1F_O-ATPase from *Acetobacterium woodii* contains F-type and V-type rotor subunits and is capable of ATP synthesis, *FEBS J.* **274**, 3421-3428.

15. Rahlfs, S., Aufurth, S. & Müller, V. (1999) The Na^+-F_1F_O-ATPase operon from *Acetobacterium woodii*. Operon structure and presence of multiple copies of *atpE* which encode proteolipids of 8- and 18-kDa, *J Biol Chem.* **274**, 33999-34004.

16. Rahlfs, S. & Müller, V. (1999) Sequence of subunit *a* of the Na^+-translocating F_1F_O-ATPase of *Acetobacterium woodii*: proposal for residues involved in Na^+ binding, *FEBS Lett.* **453**, 35-40.

17. Rahlfs, S. & Müller, V. (1997) Sequence of subunit *c* of the Na^+-translocating F_1F_O ATPase of *Acetobacterium woodii*: proposal for determinants of Na^+ specificity as revealed by sequence comparisons, *FEBS Lett.* **404**, 269-271.

18. Brandt, K. & Müller, V. (2015) Hybrid rotors in F_1F_o ATP synthases: subunit composition, distribution, and physiological significance, *Biol Chem*, in press.

19. Aufurth, S., Schägger, H. & Müller, V. (2000) Identification of subunits *a*, *b*, and c_1 from *Acetobacterium woodii* Na^+-F_1F_O-ATPase. Subunits c_1, c_2, and c_3 constitute a mixed *c*-oligomer, *J Biol Chem.* **275**, 33297-33301.

20. Fritz, M., Klyszejko, A. L., Morgner, N., Vonck, J., Brutschy, B., Müller, D. J., Meier, T. & Müller, V. (2008) An intermediate step in the evolution of ATPases: a hybrid F_1F_O rotor in a bacterial Na^+ F_1F_O ATP synthase., *FEBS J.* **275**, 1999-2007.

21. Matthies, D., Zhou, W., Klyszejko, A. L., Anselmi, C., Yildiz, Ö., Brandt, K., Müller, V., Faraldo-Gomez, J. D. & Meier, T. (2014) High-resolution structure and mechanism of Na^+-coupled F/V-hybrid ATP synthase rotor ring, *Nat Commun.* **5**, 5286.

22. Brandt, K., Müller, D. B., Hoffmann, J., Hübert, C., Brutschy, B., Deckers-Hebestreit, G. & Müller, V. (2013) Functional production of the Na^+ F_1F_O ATP synthase from *Acetobacterium woodii* in *Escherichia coli* requires the native AtpI, *J Bioenerg Biomembr.* **45**, 15-23.

23. Nishi, T., Kawasaki-Nishi, S. & Forgac, M. (2003) The first putative transmembrane segment of subunit *c*" (Vma16p) of the yeast V-ATPase is not necessary for function, *J Biol Chem.* **278**, 5821-5827.

24. Hirata, R., Graham, L. A., Takatsuki, A., Stevens, T. H. & Anraku, Y. (1997) VMA11 and VMA16 encode second and third proteolipid subunits of the *Saccharomyces cerevisiae* vacuolar membrane H^+-ATPase, *J Biol Chem.* **272**, 4795-4803.

25. Forgac, M. (2007) Vacuolar ATPases: rotary proton pumps in physiology and pathophysiology, *Nat Rev Mol Cell Biol.* **8**, 917-929.

26. Rak, M., Gokova, S. & Tzagoloff, A. (2011) Modular assembly of yeast mitochondrial ATP synthase, *EMBO J.* **30**, 920-930.

27. Brockmann, B., Koop Genannt Hoppmann, K. D., Strahl, H. & Deckers-Hebestreit, G. (2013) Time-delayed in vivo assembly of subunit *a* into preformed *Escherichia coli* F_oF_1 ATP synthase, *J Bacteriol.* **195**, 4074-4084.

28. McCarthy, J. E. (1990) Post-transcriptional control in the polycistronic operon environment: studies of the *atp* operon of *Escherichia coli*, *Mol Microbiol.* **4**, 1233-1240.

29. McCarthy, J. E., Schauder, B. & Ziemke, P. (1988) Post-transcriptional control in *Escherichia coli*: translation and degradation of the *atp* operon mRNA, *Gene.* **72**, 131-139.

30. McCarthy, J. E. (1988) Expression of the *unc* genes in *Escherichia coli*, *J Bioenerg Biomembr.* **20**, 19-39.

31. McCarthy, J. E. & Bokelmann, C. (1988) Determinants of translational initiation efficiency in the *atp* operon of *Escherichia coli*, *Mol Microbiol.* **2**, 455-465.

32. McCarthy, J. E., Schairer, H. U. & Sebald, W. (1985) Translational initiation frequency of atp genes from *Escherichia coli*: identification of an intercistronic sequence that enhances translation, *EMBO J.* **4**, 519-526.

33. Hellmuth, K., Rex, G., Surin, B., Zinck, R. & McCarthy, J. E. (1991) Translational coupling varying in efficiency between different pairs of genes in the central region of the *atp* operon of *Escherichia coli*, *Mol Microbiol.* **5**, 813-824.

34. Schauder, B. & McCarthy, J. E. (1989) The role of bases upstream of the Shine-Dalgarno region and in the coding sequence in the control of gene expression in *Escherichia coli*: translation and stability of mRNAs in vivo, *Gene.* **78**, 59-72.

35. Sambrook, J., Fritsch, E. F. & Maniatis, T. (1989) *Molecular cloning: a laboratory manual*, 2nd edn, Cold Spring Harbor Laboratory Press, Cold Spring Harbor, N.Y.

36. Klionsky, D. J., William, S. A., Brusilow, A. & Simoni, R. D. (1984) *In vivo* evidence for the role of the ε subunit as an inhibitor of the proton-translocating ATPase of *Escherichia coli*, *Journal of Bacteriology.* **160**, 1055-1060.

37. Zhou, K., Zhou, L., Lim, Q., Zou, R., Stephanopoulos, G. & Too, H. P. (2011) Novel reference genes for quantifying transcriptional responses of *Escherichia coli* to protein overexpression by quantitative PCR, *BMC molecular biology.* **12**, 18-27.

38. Mayer, F., Leone, V., Langer, J. D., Faraldo-Gómez, J. D. & Müller, V. (2012) A *c* subunit with four transmembrane helices and one ion (Na^+) binding site in an archaeal ATP synthase: implications for *c* ring function and structure, *J Biol Chem.* **287**, 39327-39337.

Figure legends

Fig. 1. Organization of the *atp* operon of *E. coli* and *A. woodii* (A) and alignment of subunits c_1 and $c_{2/3}$ (B). The N-terminal helix as well as the inner and outer transmembrane helices are shown in the alignment. The Na^+ binding motif as well as the glutamate to glutamine substitution are highlighted.

Fig. 2. Na^+ transport measurements (A), SDS gel (B) and LILBID-MS spectra (C, D) of the *c* ring purified from of the truncated c_1 variant ($c_{1æ2\text{-}18}$). (A) Proteoliposomes (protein concentration 0.2 mg/ml) containing the wild type enzyme (y) and the truncated c_1 variant (♦) in hydrolysis buffer, containing 6 mM ^{22}NaCl (0.5 µCi/ml), 17 µM Valinomycin and 40 mM K^+ transported Na^+ upon addition of ATP (5 mM). (B) The isolated *c* ring was either treated with trichloroacetic acid (TCA) to disintegrate the *c* ring or separated without TCA treatment by SDS-PAGE prior to visualization using silver staining. (C, D) The mass spectra show charge distribution of the intact *c* ring under soft LILBID conditions (C) as well as the fragments of the *c* ring under harsh conditions (D). The fragmentation of the *c* ring leads to two series of subcomplexes consisting of only $c_{2/3}$ monomers (indicated by blue vertical bars) or one c_1 and 1-9 $c_{2/3}$ subunits (indicated by red vertical bars). No subcomplex contains more than one c_1 subunit. a.u., arbitrary units.

Fig. 3. Effect of *c* subunit deletions on subunit composition of the Na^+ F_1F_o ATP synthase and ATP hydrolysis. (A, B) Membrane samples of the mutants and the wild type (10 µg) were separated by SDS-PAGE and blotted against specific antibodies against subunit *b* (A) and β (B). (C) The specific activity of the membranes of the deletion mutants is shown in comparison to the wild type. (D)The purified ATP synthase of the variants (10 µg) were separated by SDS-PAGE and stained with silver. (E)The specific activity of the purified enzyme of the deletion variants is shown in comparison to the wild type.

Fig. 4. Subunit composition and stoichiometry of the *c* rings from the heterologously produced wild type, the æc_1 variant, the **æ**c_2 variant and the **æ**c_3 variant. (A, B) The isolated *c* rings were either treated with trichloroacetic acid (TCA) to disintegrate the *c* ring or separated without TCA treatment by SDS-PAGE and the proteins were stained with silver. (C-E) LILBID anion spectra of purified *c* ring from the variants (C = æc_2, D = æc_3 , E = æc_1) under medium laser desorption conditions with the charge distribution of the fragments of the ring is shown. The fragmentation of the *c* ring leads to one series of subcomplexes consisting of one c_1 and up to nine c_3 or c_2 monomers in case of the **æ**c_2 or the **æ**c_3 variant, respectively. In case of the **æ**c_1 variant the fragmentation leads to one series of subcomplexes consisting of only $c_{2/3}$ monomers. Similiar to Fig. 2D red and blue bars indicate theoretical masses of the subcomplexes without any lipid attachments. In addition the spectrum in Fig. 4E also shows a large signal assigned to the *b* subunit - a contaminant also visible in Fig. 4A. a.u., arbitrary units.

Fig. 5. Na^+ transport of the wild type and the variants (A) and transcriptional analysis of genes from the *atp* operon of the wild type and the deletion mutants (B). (A) Proteoliposomes (protein concentration 0.2 mg/ml) of the wild type (y), æc_1 variant (♦), æc_2 variant (Ç) and the æc_3 variant (z) in hydrolysis buffer, containing 6 mM ^{22}NaCl (0.5 µCi/ml), 17 µM Valinomycin and 40 mM K^+ transported Na^+ upon addition of ATP (5 mM). (B) Relative mRNA levels were analyzed for the genes *atpB*, *atpF* and *atpD* of the wild type and the deletion mutants. The wild type was set to one.

Fig. 6. Subunit c_2 dominates over c_3 in the *c* ring of *A. woodii*. To distinguish between the F-type like *c* subunits within the *c* ring we tagged the F-type like *c* subunit c_2 or c_3 with additional alanine residues at the C-terminal end. The *c* subunits were extracted by chloroform/methanol from purified ATP synthases and analyzed by MALDI-TOF-MS.

Tab. 1. Primer used for construction of mutants.

Primer	**Sequence (5ĉ-3ĉ)**[a,b]
A.w.dE1-for	P*ATGGCTTTGTATCAACAACG
A.w.dE1-rev	P*CTCATTAATCCATCGCCCCAG
A.w.dE2-for	P*AACAGTAACGGATAGATAAT
A.w.dE2-rev	P*AACGTTGTTGATACAAAGCC
A.w.dE3-for	P*ATGGCTTTGTATCAACAACG
A.w.dE3-rev	P*CTCATTAATCCATCGCCCCAG
A.w.trE1N-for2	P*GATCCGGTTGATGTTATTAAAGGATTTTC
A.w.trE1N-rev2	P*CATACTGTTCCCCTCCTTTCTTTCTC
A.w.*atpE*$_2$+1A-for	CCCATTTTTT**GCT**TAAAAACAGTAACGGATAG
A.w.*atpE*$_2$+1A-rev	CGTTACTGTTTTTA**AGC**AAAAAATGGGTTTGC
A.w.*atpE*$_2$+2A-for	CCCATTTTTT**GCTGCA**TAAAAACAGTAACGGATAG
A.w.*atpE*$_2$+2A-rev	CGTTACTGTTTTTA**TGCAGC**AAAAAATGGGTTTGC
A.w.*atpE*$_3$+1A-for	CCAATCCTTTCTTT**GCA**TAAATTGAGGTGATTC
A.w.*atpE*$_3$+1A-rev	CACCTCAATTTA**TGC**AAAGAAAGGATTGGCAAAG

[a] Phosphorylation at 5ĉ-site of the primer are illustrated as P*.
[b] Codons for alanine are marked in bold.

Tab. 2. Primer used for quantitative real-time PCR.

Primer	**Sequence (5ĉ-3ĉ)**
A.w.RT-*atpB*-for	CATGGCTCTAATCTTGGTTGTG
A.w.RT-*atpB*-rev	CCATAGATCCCTGCAGTGTTC
A.w.RT-*atpE*$_1$-for	GAGTCAGTTTGATCCGGTTG
A.w.RT-*atpE*$_1$-rev	GCTCCTAGAAGCATAATCATCAC
A.w.RT-*atpE*$_2$-for2	GGCTTTGTATCAACAACGTTTAG
A.w.RT-*atpE*$_2$-rev2	GTTTTATCAGATAATTTATTATCTATCCGTTACTG
A.w.RT-*atpE*$_3$-for2	GATAATAAATTATCTGATAAAACAAGGAGG
A.w.RT-*atpE*$_3$-rev2	CAAGTTTTTCATTTGTGAATCACCTC
A.w.RT-*atpF*-for	GCTGAAATTGTCGGAGCTACTG
A.w.RT-*atpF*-rev	GCGTCGCTATGAGCCTTATC
A.w.RT-*atpD*-for	GCTGTGGATACAGGGTCAGC
A.w.RT-*atpD*-rev	GGTTTCAAACATTTCTGGTTGCG
A.w.RT-*bla*-for	GATGCTGAAGATCAGTTGGGTG
A.w.RT-*bla*-rev	CCAAGTCATTCTGAGAATAGTGTATGC
E.c.RT-*CysG*-for	TTGTCGGCGGTGGTGATGTC
E.c.RT-*CysG*-rev	ATGCGGTGAACTGTGGAATAAACG

Fig. 1.

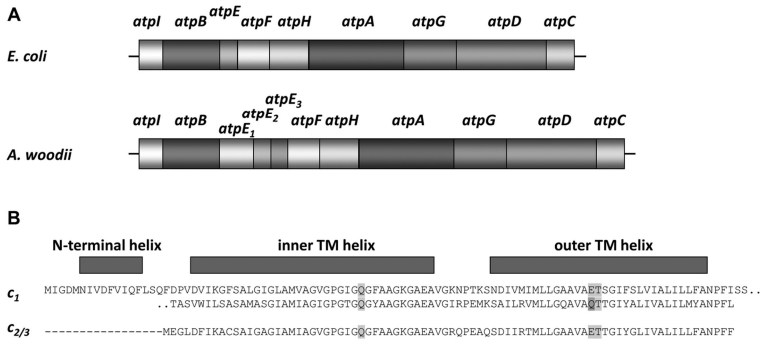
A
atpI atpB atpE atpF atpH atpA atpG atpD atpC
E. coli
atpI atpB atpE1 atpE2 atpE3 atpF atpH atpA atpG atpD atpC
A. woodii
B
N-terminal helix
inner TM helix
outer TM helix
c1 MIGDMNIVDFVIQFLSQFDPVDVIKGFSALGIGLAMVAGVGPGIGQGFAAGKGAEAVGKNPTKSNDIVMIMLLGAAVAETSGIFSLVIALILLFANPFISS..
..TASVWILSASAMASGIAMIAGIGPGTGQGYAAGKGAEAVGIRPEMKSAILRVMLLGQAVAETTGIYALIVALILMYANPFL
c2/3 ----------MEGLDFIKACSAIGAGIAMIAGVGPGIGQGFAAGKGAEAVGRQPEAQSDIIRTMLLGAAVAETTGIYGLIVALILLFANPFF

Fig. 2.

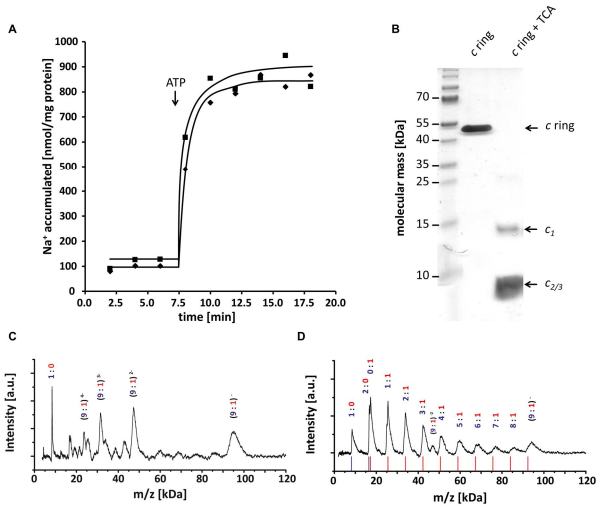
A
ATP
Na+ accumulated [nmol/mg protein]
time [min]
B
c ring
c ring + TCA
molecular mass [kDa]
c ring
c1
c2/3
C
Intensity [a.u.]
m/z [kDa]
D
Intensity [a.u.]
m/z [kDa]

Fig. 3.

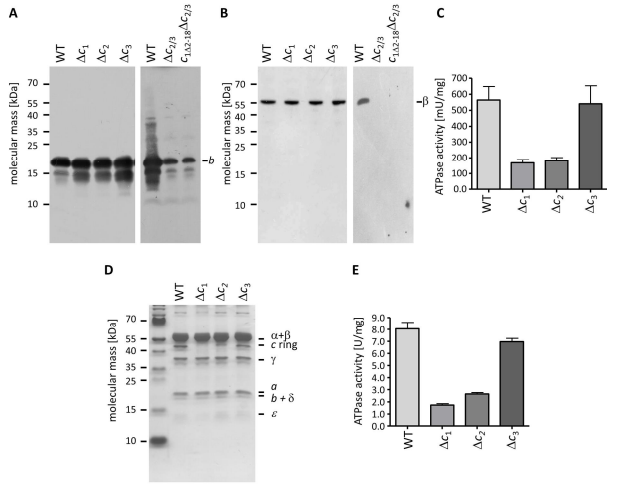
A
B
C
D
E
WT
molecular mass [kDa]
ATPase activity [mU/mg]
ATPase activity [U/mg]
α+β
c ring
γ
a
b + δ
ε

Fig. 4.

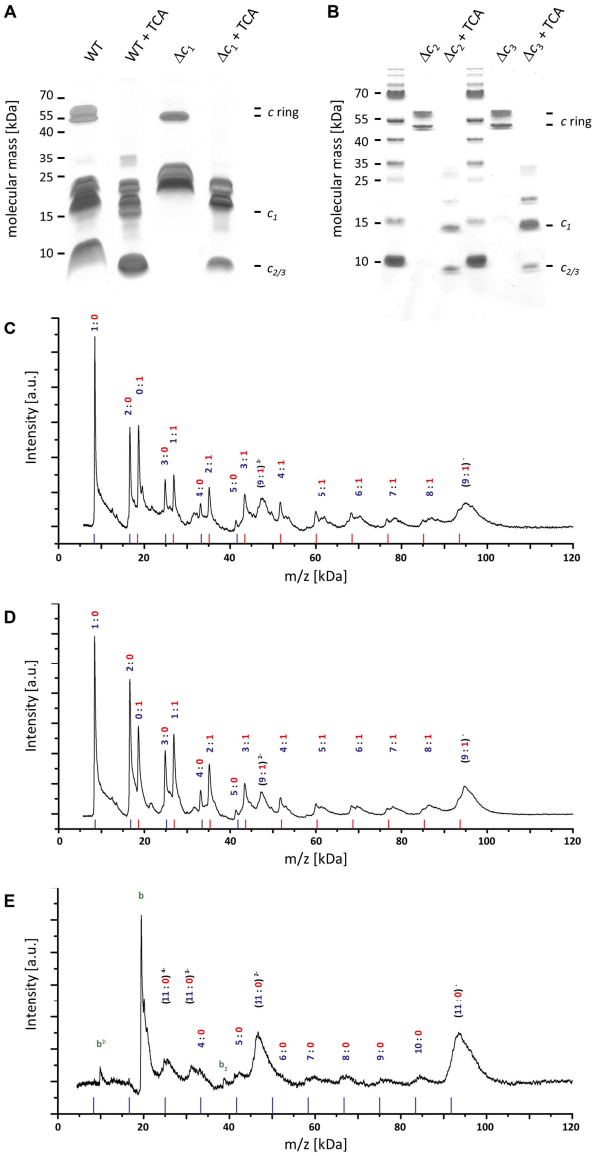
A
WT
WT + TCA
ΔC1
ΔC1 + TCA
molecular mass [kDa]
70
55
40
35
25
15
10
c ring
c1
c2/3
B
ΔC2
ΔC2 + TCA
ΔC3
ΔC3 + TCA
molecular mass [kDa]
c ring
c1
c2/3
C
Intensity [a.u.]
m/z [kDa]
D
Intensity [a.u.]
m/z [kDa]
E
Intensity [a.u.]
m/z [kDa]

Fig. 5.

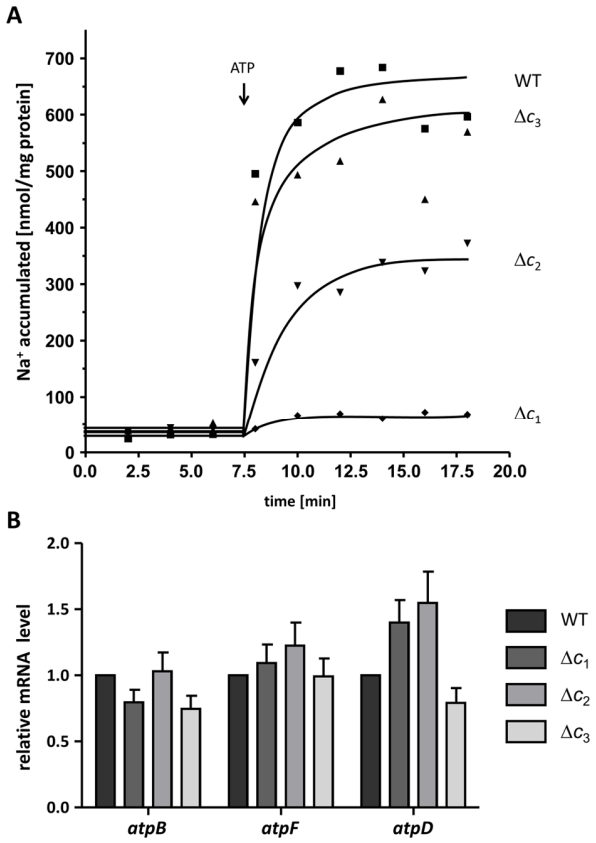
A
ATP
WT
Δc3
Δc2
Δc1
Na+ accumulated [nmol/mg protein]
time [min]
B
relative mRNA level
WT
Δc1
Δc2
Δc3
atpB
atpF
atpD

Fig. 6.

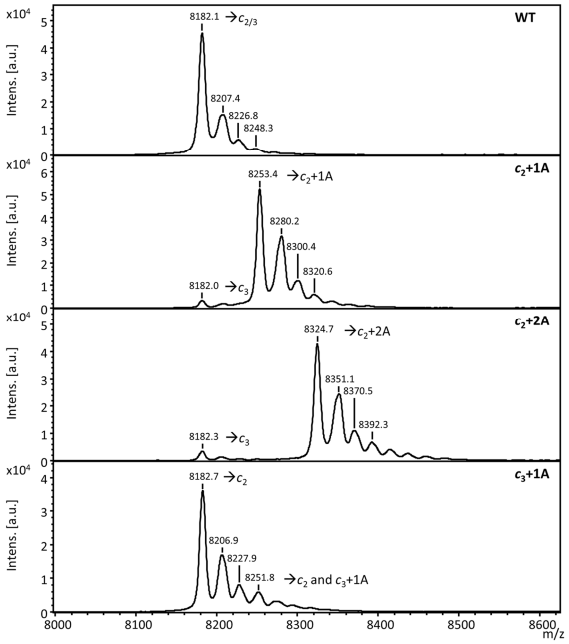
WT
8182.1 →$c_{2/3}$
8207.4
8226.8
8248.3
c_2+1A
8253.4 →c_2+1A
8280.2
8300.4
8320.6
8182.0 →c_3
c_2+2A
8324.7 →c_2+2A
8351.1
8370.5
8392.3
8182.3 →c_3
c_3+1A
8182.7 →c_2
8206.9
8227.9
8251.8 →c_2 and c_3+1A
Intens. [a.u.]
x10⁴
m/z
8000
8100
8200
8300
8400
8500
8600